FRACTURE MECHANICS OF MATERIALS UNDER COMPRESSION ALONG CRACKS (SURVEY). STRUCTURAL MATERIALS*

A. N. Guz' and V. M. Nazarenko

UDC 539.3

3. The approach elucidated for elastic highly-elastic materials can be extended to other models of a deformable body, particularly in application to the most generally used structural materials (composites, plastics, etc.) [19]. Such an extension is based on the utilization of a general approach [19] in application to different models of materials. The researches performed for the structural materials mentioned [16, 19, 20, 23-25, 27, 28, 31, 37-39, 50, 51, 53, 56, 61, 70] refer to the first group of papers* (see Sec. 1). Since the majority of structural materials are comparatively stiff and do not sustain significant deformations, the second modification of the theory of small subcritical deformations [19], when the subcritical state is defined within the framework of geometrically linear theory, is used in the investigations.

3.1. Composite Materials (Continual Model)

Formulation of the problems in application to the continual model of a composite material is given in [16, 19]. Following [19], we will consider the case when the minimal crack dimensions in the composite are substantially greater than the dimensions of its structural elements, i.e., macrocracks are considered. Fracture processes in which the properties of a piecewise-homogeneous medium appear (of the type of fracture on the interfacial boundary of media, etc.) are not examined here. Under the assumptions mentioned, a composite material can be modelled by an orthotropic (in particular, transversally isotropic) medium with the cited characteristics. Such an approach permits investigation of laminated composites because of existing initial stresses of a different nature acting along the cracks as a fracture problem for a material with plane cracks in planform under the effect of forces parallel to the plane of the crack.

A three-dimensional linearized theory of the stability of deformable bodies under small subcritical deformations [19] is used in the investigations since the majority of structural materials do not sustain large deformations. The second modification of the theory of small subcritical deformations, when the subcritical state is determined by a geometrically linear theory, is used. In this connection, no difference can be made between the coordinates of the undeformed and deformed states when using linearized equations for the stress tensor and displacement vector perturbations, as well as between the tensor components evaluated in the coordinates of the mentioned states. Consequently, by using the results of [19] it is expedient to use the coordinates of the initial strain state $y_j = \lambda_j x_j$ $(j = 1, 2, 3)$.

Let us note that as a rule the case of unequal roots of the characteristic equation is realized for composite materials. One of the fundamental features of composite materials, the reduced shear stiffness, should be taken into account in performing investigations.

The elastic relationships for a physically linear orthotropic body are

*The present paper continues the survey [A. N. Guz' and V. M. Nazarenko, " Fracture mechanics of materials under compression along cracks (survey). Highly-elastic materials," Prikl. Mekh., 25, No. 9, 3-32 (1989)] of investigations of questions for fracture under compression along cracks as applied to extensively utilized structural materials, composites with elastic components and elastic-plastic bodies. In the interest of convenience in the exposition, a single system of numbering the sections and formulas, figures, tables, as well as the bibliographic references is used (the references in this paper are given in conformity with the bibliographic listing in the above-mentioned citation).

Institute of Mechanics, Ukrainian Academy of Sciences, Kiev. Translated from Prikladnaya Mekhanika, Vol. 25, No. 10, pp. 3-19, October, 1989. Original article submitted June 1, 1988.

0038-5298/89/2510-0959$12.50

$$\sigma_{ij}^0 = \delta_{ij}A_{ik}\varepsilon_{kk}^0 + 2(1-\delta_{ij})G_{ij}\varepsilon_{ij}^0; \qquad A_{ik} = A_{ki}, \quad G_{ij} = G_{ji},$$
$$\varepsilon_{ij}^0 = \delta_{ij}a_{ik}\sigma_{kk}^0 + \frac{1-\delta_{ij}}{2G_{ij}}\sigma_{ij}^0, \quad a_{ik} = a_{ki}, \tag{3.1.1}$$

where A_{ij} are elasticity coefficients, a_{ij} are pliability coefficients (A_{ij}, a_{ij} are the reduced characteristics of the continual model of the composite).

With the application of engineering constants

$$\varepsilon_{11}^0 = \frac{1}{E_1}\sigma_{11}^0 - \frac{\nu_{21}}{E_2}\sigma_{22}^0 - \frac{\nu_{31}}{E_3}\sigma_{33}^0; \qquad \varepsilon_{12}^0 = \frac{1}{2G_{12}}\sigma_{12}^0; \qquad \varepsilon_{22}^0 = -\frac{\nu_{12}}{E_1}\sigma_{11}^0 +$$
$$+\frac{1}{E_2}\sigma_{22}^0 - \frac{\nu_{32}}{E_3}\sigma_{33}^0; \qquad \varepsilon_{13}^0 = \frac{1}{2G_{13}}\sigma_{13}^0;$$
$$\varepsilon_{33}^0 = -\frac{\nu_{13}}{E_1}\sigma_{11}^0 - \frac{\nu_{23}}{E_2}\sigma_{22}^0 + \frac{1}{E_3}\sigma_{33}^0; \qquad \varepsilon_{23}^0 = \frac{1}{2G_{23}}\sigma_{23}^0; \qquad \frac{\nu_{21}}{E_2} = \frac{\nu_{12}}{E_1}, \tag{3.1.2}$$
$$\frac{\nu_{31}}{E_3} = \frac{\nu_{13}}{E_1}, \qquad \frac{\nu_{32}}{E_3} = \frac{\nu_{23}}{E_2}.$$

In the case of transversally-isotropic bodies for which the isotropy plane agrees with the plane x_1Ox_2,

$$\varepsilon_{11}^0 = \frac{1}{E}(\sigma_{11}^0 - \nu\sigma_{22}^0) - \frac{\nu'}{E'}\sigma_{33}^0; \qquad \varepsilon_{12}^0 = \frac{1}{2G}\sigma_{12}^0; \qquad G = \frac{E}{2(1+\nu)};$$
$$\varepsilon_{22}^0 = \frac{1}{E}(-\nu\sigma_{11}^0 + \sigma_{22}^0) - \frac{\nu'}{E'}\sigma_{33}^0; \qquad \varepsilon_{13}^0 = \frac{1}{2G'}\sigma_{13}^0;$$
$$\varepsilon_{33}^0 = -\frac{\nu'}{E'}(\sigma_{11}^0 + \sigma_{22}^0) + \frac{1}{E'}\sigma_{33}^0; \qquad \varepsilon_{23}^0 = \frac{1}{2G'}\sigma_{23}^0; \qquad A_{11} = A_{22}, \tag{3.1.3}$$
$$A_{13} = A_{23}, \qquad G' = G_{13} = G_{23}, \qquad A_{11} - A_{12} = 2G_{12};$$
$$G = G_{12}; \qquad E = E_1; \qquad E' = E_3.$$

Cracks in an Infinite Composite Material Arranged in One Plane. Plane (under uniaxial compression) and spatial (under biaxial uniform compression) problems on the compression of a composite along a finite number of cracks disposed in one plane are investigated in the papers [16, 19]. The initial stage of fracture is in the nature of a surface instability and is determined by loads corresponding to a surface instability of a half-space.

The equation to determine the critical load in the case of plane problems has the form [16, 19] (the cracks are in the plane y_2 = const)

$$x^3\left[\frac{A_{22}}{A_{11}}\left(\frac{A_{22}}{A_{11}} - \varepsilon\right)\right] + x^2\left[\frac{A_{22}}{A_{11}}\left(\frac{A_{22}}{A_{11}}\varepsilon + 2\frac{A_{22}}{A_{11}} - 2\frac{A_{12}^2}{A_{11}^2} - \varepsilon\right)\right] +$$
$$+x\left[\left(\frac{A_{22}}{A_{11}} - \frac{A_{12}^2}{A_{11}^2}\right)\left(\frac{A_{22}}{A_{11}} - \frac{A_{12}^2}{A_{11}^2} + 2\frac{A_{22}}{A_{11}}\varepsilon\right)\right] + \left[\varepsilon\left(\frac{A_{22}}{A_{11}} - \frac{A_{12}^2}{A_{11}^2}\right)^2\right] = 0, \tag{3.1.4}$$
$$x \equiv \frac{\sigma_{11}^0}{A_{11}}, \qquad \varepsilon \equiv \frac{G_{12}}{A_{11}}.$$

Taking account of the reduced shear stiffness of the material ($\varepsilon \ll 1$), the critical load can be determined approximately from (3.1.4)

$$\frac{(\sigma_{11}^0)^*}{A_{11}} \approx -\frac{G_{12}}{A_{11}}\left[1 - \frac{G_{12}^2}{A_{11}A_{22}}\frac{A_{11}^2A_{22}^2}{(A_{11}A_{22} - A_{12}^2)^2}\right], \tag{3.1.5}$$

or in the engineering constants of an orthotropic body for the reduced characteristics of the composite

$$(\sigma_{11}^0)^* \approx -G_{12}\left[1 - \frac{G_{12}^2}{E_1E_2}(1-\nu_{13}\nu_{31})(1-\nu_{23}\nu_{32})\right]. \tag{3.1.6}$$

The equation to determine the critical load in the case of spatial (uniform biaxial compression) problems has the form [19] (the composites with reduced characteristics of a

transversally-isotropic body, cracks disposed in the plane of isotropy)

$$x^3\left[\frac{A_{33}}{A_{11}}\left(\frac{A_{33}}{A_{11}}-\varepsilon\right)\right]+x^2\left[\frac{A_{33}}{A_{11}}\left(\frac{A_{33}}{A_{11}}\varepsilon+2\frac{A_{33}}{A_{11}}-2\frac{A_{13}^2}{A_{11}^2}-\varepsilon\right)\right]+$$

$$+x\left[\left(\frac{A_{33}}{A_{11}}-\frac{A_{13}^2}{A_{11}^2}\right)\left(\frac{A_{33}}{A_{11}}+2\frac{A_{33}}{A_{11}}\varepsilon-\frac{A_{13}^2}{A_{11}^2}\right)\right]+\left[\varepsilon\left(\frac{A_{33}}{A_{11}}-\frac{A_{13}^2}{A_{11}^2}\right)^2\right]=0, \tag{3.1.7}$$

$$x\equiv\sigma_{11}^0/A_{11},\quad \varepsilon\equiv G_{13}/A_{11}.$$

Taking account of the reduced shear stiffness of the composite material relative to the shear of planes parallel to the plane of isotropy $y_3 = 0$ in which the cracks are arranged ($E >> G'$, $E >> E'$), we determine the critical value of the load (in engineering constants) as follows

$$(\sigma_{11}^0)^* \approx -G'\left[1-\frac{(G')^2}{EE'}(1-\nu^2)(1-\nu'\nu'')\right]. \tag{3.1.8}$$

Let us note that the approximate formula (3.1.8) is sufficiently efficient even for comparatively small values of E/G'. Thus, the exact solution of (3.17) and approximate [formula (3.1.8)] critical values of the dimensionless compressive stress $(\sigma_{11}^0)^*/E$ (E is the elastic modulus in the isotropy plane) are given in Table 4 [27] for a laminar composite with isotropic layers with Young's moduli $E^{(1)}$ and $E^{(2)}$ and Poisson ratios $\nu^{(1)} = \nu^{(2)} = 0.3$, respectively, for a bulk concentration $c_1 = 0.3$ of a material with modulus $E^{(1)}$.

Surface Lamination of Composites under Compression along Near-Surface Macrocracks. Problems on the biaxial uniform compression of a composite along a near-surface circular crack in an axisymmetric formulation are investigated in detail in [27, 50, 51, 53] within the framework of the continual model of a composite (see above). Using the Hankel transform apparatus, the problems are reduced to a system of dual integral equations and then by application of the Uflyand method [72] to a system of integral equations with an additional condition (2.2.12) (for the case of unequal roots of the characteristic equation). The quantities n_1^0, n_2^0, ℓ_1^0, ℓ_2^0, m_1^0, m_2^0, k_1, k_2, k are determined in terms of the reduced composite characteristics with simplifications characteristic for the second modification of the theory of small subcritical deformation [19] taken into account. Numerical investigations are performed for composites with reduced characteristics of a transversally-isotropic medium.

Laminar Composite with Isotropic Layers. A transversally-isotropic medium is in the macrovolumes [44]. A macrocrack is in the plane of isotropy parallel to the layer of interfacial surfaces as well as the free surface. The dependences of the critical dimensionless compressive stresses σ, $\bar{\sigma}$ (compressions σ_{11}^0 referred, respectively, to the critical compressive stress for a surface instability $(\sigma_{11}^0)^*$ and the reduced elastic modulus E in the plane of isotropy) on the ratio between the elastic moduli of the isotropic layers with identical Poisson ratios are presented in Fig. 24. The curves 1 are constructed for values of the relative distance from the lamination to the boundary surface $\beta = h\alpha^{-1} = 1/8$, and curves 2 for $\beta = 1/4$. The critical compression $\sigma(\bar{\sigma})$ grows (decreases) monotonically as the ratio between the layer elastic moduli $E^{(1)}/E^{(2)}$ grows. Compared with the case of an isolated crack in an infinite material [19], the critical compressive stress σ_{11}^0 can diminish by more than one order for the considered values of β, depending on the relationships of the elastic characteristics.

According to the approximate approach, the critical load corresponds in this case to the Euler critical load for a circular slab (slab radius equal to the lamination radius and the thickness to the distance from the lamination to the free surface) under clamping conditions from stiff framing to simple support. The dashed lines 3 and 5 in Fig. 24b correspond to the dimensionless Euler compressive stress $\bar{\sigma}_{E1} = \sigma_0^*/E$ for simple support for the values $\beta = 1/8$ and 1/4 and the dash-dot lines 4 and 6 to stiff clamping for the same values of β. The Euler critical compressive stress for stiff framing or simple support yields a substantial error as compared with the critical compressive stress value obtained in [27] (for certain relationships between the composite elastic characteristics, the mentioned values can differ by more than twice).

The dependence of the relative critical shortening $\varepsilon_1 = (1 - \lambda_1)$ on ν for a laminar composite with identical Poisson ratios $\nu^{(1)} = \nu^{(2)} = \nu$ is represented in Fig. 25 [50] for

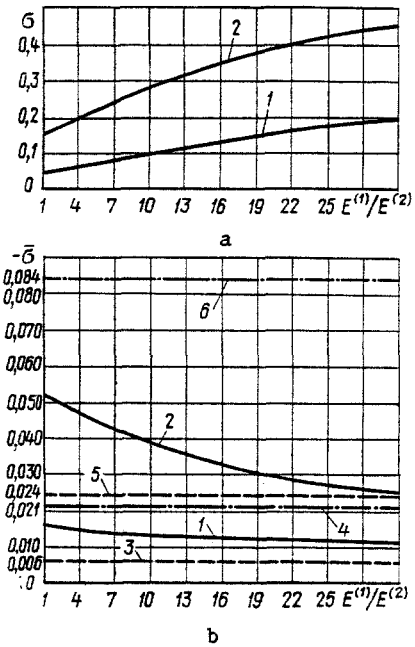

Fig. 24

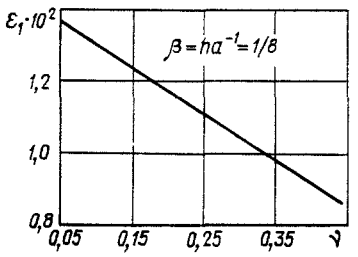

Fig. 25

TABLE 4

$E^{(1)}/E^{(2)}$	E/G'	Exact value	Approximate value
1	2,600	—0,3308	—0,3375
4	3,828	—0,2386	—0,2408
7	5,408	—0,1743	—0,1751
10	7,023	—0,1364	—0,1367
13	8,648	—0,1117	—0,1119
16	10,278	—0,0946	—0,0947
19	11,911	—0,0820	—0,0820
22	13,545	—0,0723	—0,0724
25	15,180	—0,0647	—0,0647
28	16,815	—0,0585	—0,0585
31	18,452	—0,0534	—0,0534

TABLE 5

$\beta=h\alpha^{-1}$	1/8		1/4	
N	ε_1	σ_{11}^0/E	ε_1	σ_{11}^0/E
2	0,008	—0,0114	0,024	—0,0346
3	0,009	—0,0127	0,025	—0,0351
4	0,006	—0,0092	0,023	—0,0337
5	0,006	—0,0092	0,023	—0,0337
6	0,006	—0,0092	0,023	—0,0337

the ratio $E^{(1)}/E^{(2)} = 3$ between the layer elastic moduli and concentration $c_1 = 0.3$ of the layers with modulus $E^{(1)}$.

The results for a specific laminar composite, aluminoboron silicate glass with an epoxy-maleic resin, are represented in Fig. 26: the dependence of σ, $\bar{\sigma}$ on the glass concentration c_1. Curves 1 and 2 correspond to the values $\beta = 1/8$ and $1/4$. The critical compressive stress depends substantially on the glass concentration (for $\beta = 1/8$ and the σ, $\bar{\sigma}$ differ threefold for $c_1 = 0$ and $c_1 = 0.5$) [27].

Composites with Stochastic Bonding in the Plane $y_3 = \text{const}$ by Short Ellipsoidal Fibers. A transversally-isotropic medium with isotropy plane $y_3 = \text{const}$ is in the macrovolumes [44]. The dependences $\varepsilon_1 = \varepsilon_1(\beta)$ and $\bar{\sigma} = \bar{\sigma}(\beta)$ of the relative critical shortening and the critical dimensionless compressive stress on the relative distance β from the macrocrack to the free boundary are presented in Fig. 27 for a carbon plastic bonded by carbon fibers for a $c_1 = 0.7$ fiber concentration and a ratio 10 between the longitudinal and transverse fiber dimensions [50]. The macrocharacteristics of the carbon plastic are taken from [43], and ε_1, $\bar{\sigma}$ tend asymptotically to the values 0.085 and -0.097 as $\beta \to \infty$, corresponding to the case of an isolated crack in an infinite material. For $\beta \geq 4$ the critical compressive stress differs from that for the isolated crack in an infinite material by less than 5%. The dimensionless Euler critical compressive stress $\bar{\sigma}_{E1} = \sigma_0^*/E$ calculated within the framework of the approximate approach for stiff clamping or simple support yields a substantial error even for comparatively small values of β (thus, for stiff clamping for $\beta = 0.25$, $\bar{\sigma}_{E1} = -0.078$, $\bar{\sigma} = -0.032$, i.e., these values differ by approximately 2.5 times).

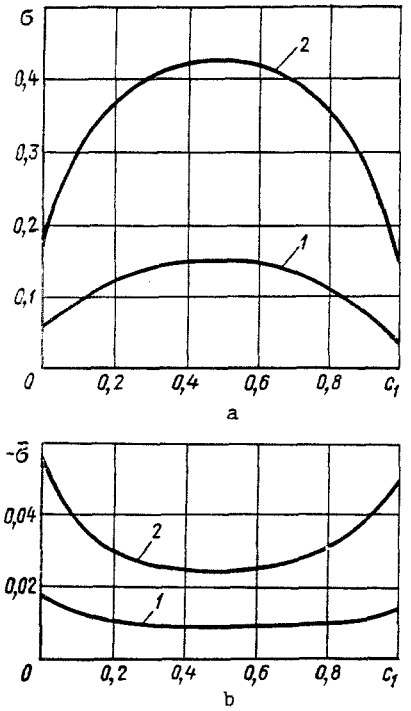

Fig. 26

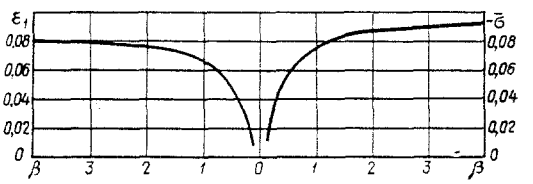

Fig. 27

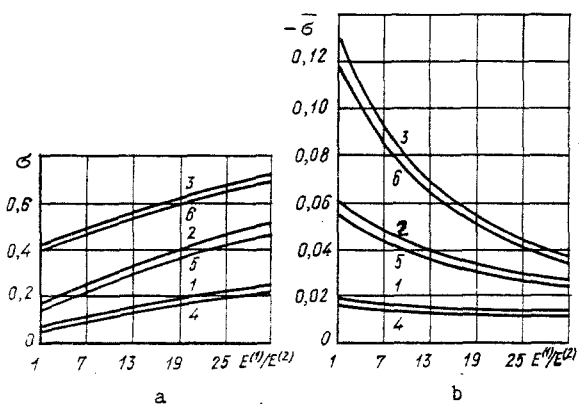

Fig. 28

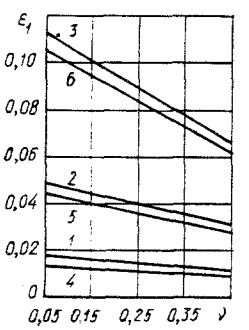

Fig. 29

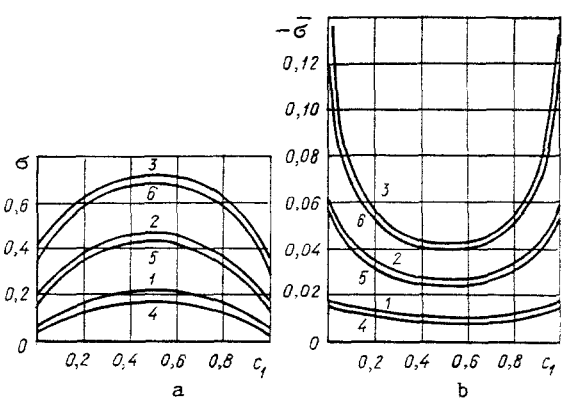

Fig. 30

Computations for a composite with reduced characteristics of the transversally-isotropic medium $\nu = 0.3$, $\nu' = 0.2$, $G'/E = 0.1$, $E'/E = 0.5$ are given in Table 5 [51]. Here, N is the number of coordinate functions being used.

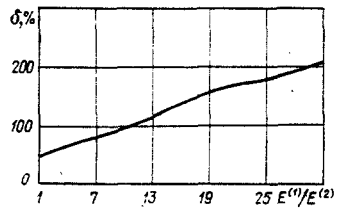

Fig. 31

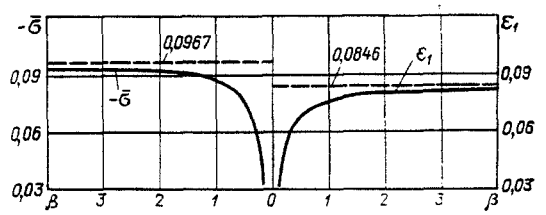

Fig. 32

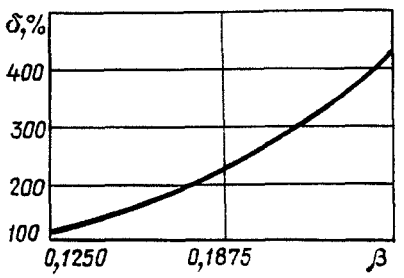

Fig. 33

Composite Lamination under Compression along Two Interior Parallel Circular Macrocracks. Biaxial uniform compression of a composite along two coaxial circular parallel cracks is examined in [23, 24, 37]. By using the zeroth order Hankel transforms and the method of [72], axisymmetric problems are reduced, separately for the bending and symmetric buckling modes, to eigenvalue problems for systems of integral equations with the additional condition (2.2.12) with the kernels (2.2.22) (taking account of simplifications utilized for the second modification of the theory of small subcritical deformations). Numerical investigations are performed for composites with reduced characteristics of the transversally-isotropic medium for the same modifications for which the investigation of the near-surface lamination of composites was performed.

Laminar Composite with Isotropic Layer. Dependences of the dimensionless critical parameters σ, $\bar{\sigma}$, ε_1 on the stiffness characteristics and component concentrations of the laminar composite are shown in Figs. 28-30. The dependences 1, 2, 3 are obtained for interior lamination with values $\beta = h a^{-1}$ (2h is the distance between the cracks, and a is their radius) equal to 1/16, 1/8, 1/4; the dependences 4, 5, 6 are for near-surface lamination for relative distances $\beta = h a^{-1}$ equal to 1/8, 1/4, 1/2 between the lamination and the free surface (h is the distace from the crack to the boundary and a is the crack radius).

The dependences of σ, $\bar{\sigma}$ on the ratio $E^{(1)}/E^{(2)} \geq 1$ between the layer elastic moduli are displayed in Figs. 28a and b (for layer Poisson ratios $\nu^{(1)} = \nu^{(2)} = 0.3$ and concentration $c_1 = 0.3$ for layers with modulus $E^{(1)}$).

For a composite with the layer Poisson ratios $\nu^{(1)} = \nu^{(2)} = \nu$, the dependences $\varepsilon_1 = \varepsilon_1(\nu)$ are presented in Fig. 29 (for $E^{(1)}/E^{(2)} = 3$ and $c_1 = 0.3$).

The dependences of σ and $\bar{\sigma}$ on the glass concentration c_1 are illustrated in Figs. 30a and b for the alumino-boron silicate glass-epoxy-maleic resin composite.

The change in the error when using approximate computational schemes $\sigma = |\bar{\sigma} - \bar{\sigma}_{E1}| / |\bar{\sigma}| \cdot 100\%$ with the change in the ratio $E^{(1)}/E^{(2)}$ (for stiff clamping) is shown in Fig. 31 for $\beta = 1/8$.

Composite with Stochastic Bonding by Short Ellipsoidal Fibers in the y_3 = const Plane. The dependences of ε_1, $\bar{\sigma}$ on β are represented in Fig. 32 for a carbon plastic bonded by finite carbon fibers (the fiber concentration is $c_1 = 0.7$ and the ratio between the longitudinal and transverse fiber dimensions is 10). The dependence of the error δ, calculated in the same manner as in the case of a composite with isotropic layers, on the quantity β is shown in Fig. 33.

Taking account of mutual crack interaction and the mutual influence of the cracks and the free boundary results in a substantial reduction in the critical compressive stresses, as compared with those obtained for an infinite composite material with an isolated crack. The critical compressive stresses obtained for interior laminations are above the critical stresses

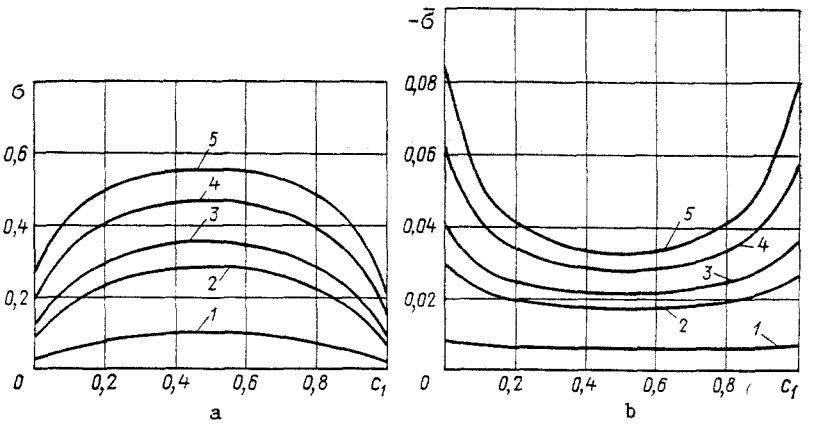

Fig. 34

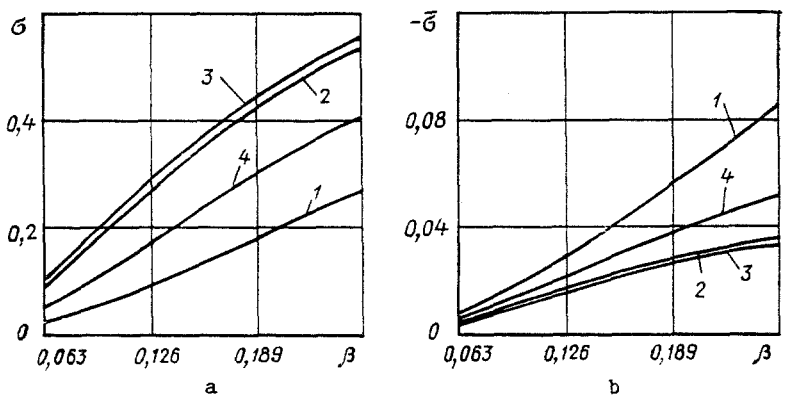

Fig. 35

for near-surface lamination. In the cases considered of changes in the stiffiness properties of the materials and the geometric parameters (β) this difference is up to 35%. The values obtained from the critical loads differ substantially from the values given by the approximate computational schemes, for instance, the Euler critical compressive stress for a circular slab calculated by interior laminations or near-surface lamination and a free boundary, yield errors of 18-66%, 52-210%, 150-770% for β equal to 0.0625, 0.125, 0.25, respectivly (interior lamination), 25-96%, 60-240%, 175-810% for β values of 0.125, 0.25, 0.5 (near-surface lamination) under stiff clamping conditions, depending on the ratio between the elastic moduli of the isotropic layers of the laminar composite.

Composite Compression along Periodically Arranged Parallel Laminations. The mentioned axisymmetric problem (for biaxial uniform compression) is examined in [31]. Applying the Hankel transform and the method of [73], the problem is reduced to eigenvalue problems for a homogeneous integral equation, (2.2.25), (2.2.27) or (2.2.25), (2.2.28), separately for the bending and symmetric buckling modes (simplifications are made in application to the second modification of the theory of small subcritical deformations). The numerical investigation is by the Bubnov–Galerkin method. Considered as an example is a laminar composite with isotropic layers, alumino-boron-glass in a composition with epoxy-maleic resin [44]. Laminations of radius a are in the isotropy planes parallel to the layer interfacial boundaries separated by a distance 2h from each other.

Dependences of the critical dimensionless compressive stresses σ, $\bar{\sigma}$ (see above) on the glass concentration c_1 are represented in Figs. 34a and b, respectively, for values of $\beta = ha^{-1}$ equal to 0.0625, 0.125, 0.15, 0.20, 0.25 (curves 1, 2, 3, 4, 5). Dependences of σ, $\bar{\sigma}$ on the relative half-distance between the cracks β for several values of the bulk concentration c_1 (0, 0.3, 0.6, 0.9) of the glass (curves 1, 2, 3, 4) are represented in Figs. 35a and b.

Comparison of the critical values $\bar{\sigma}$ for the case of a periodic arrangement of macrocracks with the cases of two interior parallel macrocracks and a near-surface macrocrack (see above) as well as values of $\bar{\sigma}$ obtained within the framework of approximate computational schemes of the stiffly clamped (simply supported) plate type, is given in Fig. 36 for a suf-

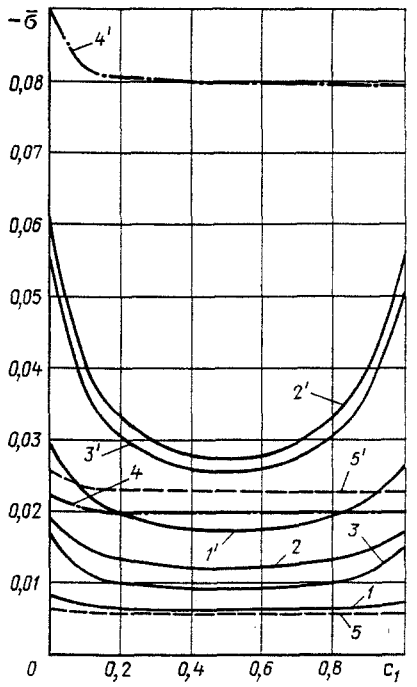

Fig. 36

ficiently small value of the relative half-distance between the cracks $\beta = 0.0625, 0.125$. The comparison was made for identical relative distances between the cracks (a periodic system of cracks, two parallel cracks) or between the crack and the free surface of the material (near-surface crack). Curves 1, 2, 3 correspond to a periodic system of cracks, two parallel cracks, and a near-surface crack. The lines 4 and 5 yield critical values calculated within the framework of approximate computational schemes for stiff clamping and simple support. The curves denoted by numbers without primes correspond to the value $\beta = 0.0625$ and with the primes to $\beta = 0.125$.

Analysis of the results of investigations that are represented graphically in Figs. 34-36 permits making the following deductions. Taking account of the macrocrack mutual influence results in a substantial reduction (by an order) in the critical compressive stresses corresponding to the beginning of fracture in comparison to their values in the case of an isolated crack in an infinite material [19]. Application of approximate computational schemes of the stiffly clamped (simply supported) plate type can result in substantial error even for comparatively extensive macrocracks (for a ratio of 1/8, 1/16 for the thickness of the connector between the cracks to their diameter). Thus, depending on the bulk concentration of glass c_1 the difference in the magnitudes of $\bar{\sigma}$ as compared with quantities obtained within the framework of the most frequently utilized approximate scheme of the stiffly clamped plate type is 170-230%, $\beta = 0.0625$; 200-370%, $\beta = 0.125$ for a periodic system of cracks, 35-120%, $\beta = 0.0625$; 60-215%, $\beta = 0.125$ for a near-surface crack, 17-67%, $\beta = 0.0625$; 45-190%, $\beta = 0.125$ for two interior parallel cracks.

All the results presented in Figs. 34-36 for a periodic system of cracks are obtained for the bending buckling mode (for the symmetric mode the critical loads turned out to be higher and, consequently, are not presented). The critical loads found characterize the beginning of fracture of a composite with periodically arranged parallel macrocracks under compression along the cracks. In the case under consideration when the bending buckling mode is realized, the critical loads obtained will also evidently characterize the subsequent total fracture of the material in the whole domain occupied by the cracks since a phenomenon occurs here that is to a definite degree analogous to the appearance of a plastic hinge over the whole thickness of the material in the beam bending case. A different situation is obtained in the case of the near-surface crack or a finite number of interior (particularly, two parallel) cracks when local buckling results just in local fracture in the crack domain (interlayer between the crack and the free surface, etc.), and the question of fracture of the whole material requires further investigation.

The above elucidation also visibly clarifies the fact that the results for a periodic system of macrocracks turn out to be closer to the results obtained within the framework of

approximate computational schemes for precisely a simply supported plate than for one stiffly clamped in contrast to the results for near-surface cracks or two parallel interior cracks.

In conclusion, let us note that the critical loads for a periodic system of parallel macrocracks yield a lower bound for the critical loads for a finite number of equidistant cracks while the loads for two parallel cracks yield the upper bound.

3.2. Plastic Materials. The general formulation of problems in application to plastic materials is given in [19]. Plastic fracture is understood to be the fracture process for which deformation beyond the elastic limit occurs in the whole material prior to fracture. The generalized conception of continuing loading formulated for a three-dimensional linearized theory of elastic-plastic media is used in considering the stability of the deformation process. Fracture mechanisms associated with the material microstructure are not considered here. The crack dimensions are assumed significantly greater than the dimensions of the characteristic microstructures (grains, crystals, etc.) existing in the material, i.e., macrocracks are considered. The second modification of the theory of small subcritical deformations when the subcritical state is determined by geometrically linear theory is used in the investigations. Coordinates of the initial deformed state y_j and components of the nonsymmetric stress perturbation tensor $\tilde{Q}_{ij}$ referred to unit area of the initial deformed state are used. Mainly the case of complex unequal roots of the characteristic equation (complex conjugate roots) is realized for plastic materials. Incompressible plastic materials are examined.

Macrocracks in an Infinite Plastic Material Arranged in One Plane. Investigations of plane (under uniaxial compression) and spatial (under biaxial uniform compression) problems for a finite number of cracks in one plane are performed in [19] in application to plastic materials. The problems reduce to problems for a half-space for the bending and symmetric buckling modes separately.

Complex potentials, introduced for plane linearized problems [19], as well as methods of Riemann–Hilbert problems are used in plane problem investigations. The results are made specific in application to the model of an incompressible isotropic elastic-plastic body within the framework of the theory of small elastic-plastic deformations. It is established that buckling of the equilibrium state of the surface instability type occurs during compression along a plane in which an arbitrary number of cracks is disposed for the fracture mechanism taken in the case of plastic fracture. Moreover, the bending and symmetric buckling modes yield the identical critical value of the compressive load determined from the equation

$$x^3 + \frac{8}{3}x^2\varepsilon + \frac{8}{9}x\varepsilon(1+2\varepsilon) + \frac{16}{27}\varepsilon^2 = 0, \tag{3.2.1}$$

where $x = \sigma_{11}/E_c$, $\varepsilon = E_k/E_c$, E_c, E_k are the secant and tangent moduli on the "stress intensity σ_u^0 ~ strain intensity ε_u^0" diagram.

The conditions $x = \sigma_{11}^0/E_c < 1$, $\varepsilon = E_k/E_c < 1$ are satisfied for structural materials. Consequently, by discarding quantities of order ε^3, an expression is obtained from (3.2.1) to determine the minimal negative roots in absolute value that corresponds to the critical load [19]

$$x^* \approx -\frac{2}{3}\varepsilon\left(1 - \frac{1}{2}\varepsilon\right), \tag{3.2.2}$$

or

$$(\sigma_{11}^0)^* \approx -\frac{2}{3}E_k\left(1 - \frac{1}{2}\frac{E_k}{E_c}\right). \tag{3.2.3}$$

In the case of biaxial uniform compression, the critical loads are determined as the least negative root, in absolute value, for the equation

$$x^3 + 2x^2\frac{1}{3}(1+3\varepsilon) + x\frac{1}{3}(1+3\varepsilon)(1+\varepsilon) + \frac{1}{27}(1+3\varepsilon)^2 = 0,$$
$$x = \sigma_{11}^0/E_c, \qquad \varepsilon = E_k/E_c. \tag{3.2.4}$$

Expanding the solution of (3.2.4) in a series in ε and keeping terms up to ε^2 inclusive, we obtain the approximate formula

TABLE 6

ε	0,1	0,2	0,3	0,4	0,5	0,6	0,7	0,8	0,9	1,0
x_T^*	—0,176	—0,204	—0,228	—0,247	—0,263	—0,275	—0,285	—0,293	—0,299	—0,304
x_a^*	—0,176	—0,204	—0,227	—0,246	—0,260	—0,268	—0,272	—0,271	—0,266	—0,255

$$x^* \approx -0{,}143 - 0{,}354\varepsilon + 0{,}242\varepsilon^2. \tag{3.2.5}$$

The exact solution x_T^* of (3.2.4) and the approximate solution x_a^* [on the basis of (3.2.5)] are presented in Table 6 for different values of ε. Comparison shows that the approximate formula (3.2.5) describes the solution well for small values for ε and yields a reduced value of x^* for ε close to one (for $\varepsilon \leq 0.7$ the difference between the exact and approximate values is less than 5%).

Fracture of Plastic Materials under Compression along Near-Surface Macrocracks. Axisymmetric problems of plastic material fracture under biaxial uniform compression along circular near-surface macrocracks were investigated in [28, 56, 61]. The investigations were performed on the basis of using a generalization of apparatus developed earlier for real unequal roots and real function to the case of complex-conjugate roots of the characteristic equation and complex-valued potential functions φ_i, $i = 1, 2$, respectively, in whose terms the stress tensor and displacement vector perturbation components are represented in the axisymmetric case [19, 28]

$$u_N = \frac{\partial}{\partial N}\operatorname{Re}(\varphi_1 + \varphi_2) \text{ etc.}$$
$$\tilde{Q}_{33} = c_{44}\operatorname{Re}\left[(1+m_1)\,l_1\frac{\partial^2\varphi_1}{\partial z_1^2} + (1+m_2)\,l_2\frac{\partial^2\varphi_2}{\partial z_2^2}\right] \text{ etc.}, \tag{3.2.6}$$

Here $\partial/\partial N$ and $\partial/\partial S$ are derivatives along the normal and the tangent in an arbitrary cylindrical coordinate system, the complex quantities m_j, l_j ($j = 1, 2$) are determined in terms of the components of the tensor $\tilde{\varkappa}$, which are determined, in turn, by the choice of the theory of plasticity. The complex variables z_i

$$z_i = w_i y_3, \quad w_i = n_i^{-1/2}, \quad \operatorname{Re} w_i > 0 \quad (i = 1, 2), \tag{3.2.7}$$

are introduced in the representations (3.2.6), where n_i are roots of the characteristic equation. The functions φ_i are here analytic in z_i and they satisfy the equations

$$\left(\frac{\partial^2}{\partial y_1^2} + \frac{\partial^2}{\partial y_2^2} + \frac{\partial^2}{\partial z_i^2}\right)\varphi_i = 0. \tag{3.2.8}$$

The representation of the potential functions φ_i in the form of integral expansions in particular complex-valued solutions of (3.2.8) (in the form of the Hankel transform in the radial coordinate) is used in solving the problems.

Each of the boundary conditions or the continuity conditions can be represented as

$$\operatorname{Re}\int_0^\infty F(A(\lambda), B(\lambda), \ldots, \lambda, r)\,d\lambda = 0 \quad (r \in I), \tag{3.2.9}$$

where F is a certain complex-valued function, I is a finite or infinite interval, $A(\lambda)$, $B(\lambda)$, ... are unknown functions of the real variable λ introduced in the integral representation for φ_i. Considering the functions $A(\lambda)$, $B(\lambda)$, ... complex-valued, we require compliance with

$$\int_0^\infty F(A(\lambda), B(\lambda), \ldots, \lambda, r)\,d\lambda = 0 \quad (r \in I), \tag{3.2.10}$$

instead of (3.2.9), from which (3.2.9) will also follow.

Together with the formal agreement between the representations of the functions φ_i in the form of Hankel integral transforms in the radius and the representations for the case of real unequal roots of the characteristic equation, the latter considerations afford the possibility of using the formalism developed for the real roots to obtain a system of resolving integral equations. The kernels and the desired functions of the system of integral equations being obtained are here complex-valued functions of real variables. In dimensionless form the resolving system of equations with an additional condition has the form [28, 56]

$$f(\xi)+\frac{s_1}{\pi s}\int_0^1 M_1(\xi,\eta)f(\eta)\,d\eta-\frac{2s_1}{\pi s}\int_0^1 N_1(\xi,\eta)g(\eta)\,d\eta=0,$$

$$g(\xi)+\frac{s_2}{\pi s}\int_0^1 M_2(\xi,\eta)g(\eta)\,d\eta-\frac{2s_2}{\pi s}\int_0^1 N_2(\xi,\eta)f(\eta)\,d\eta-\text{const}=0, \tag{3.2.11}$$

$$\int_0^1 g(\xi)\,d\xi=0;\qquad 0\leqslant\xi\leqslant 1;\qquad 0\leqslant\eta\leqslant 1;$$

$$M_1(\xi,\eta)=R_1(\eta+\xi)-R_1(1+\xi)+R_1(\eta-\xi)-R_1(1-\xi);$$

$$N_1(\xi,\eta)=S_1(\eta+\xi)+S_1(\eta-\xi),\qquad M_2(\xi,\eta)=S_2(\eta+\xi)+S_2(\eta-\xi);$$

$$N_2(\xi,\eta)=R_2(\eta+\xi)-R_2(1+\xi)+R_2(\eta-\xi)-R_2(1-\xi);$$

$$R_1(\zeta)=2s^{-1}\left\{2s_2K_0(\beta_1+\beta_2,\zeta)-\frac{1}{2}(s_1+s_2)[s_2s_1^{-1}K_0(2\beta_2,\zeta)+K_0(2\beta_1,\zeta)]\right\};$$

$$S_1(\zeta)=s^{-1}(s_1+s_2)\left\{K_1(\beta_1+\beta_2,\zeta)-\frac{1}{2}[K_1(2\beta_1,\zeta)+K_1(2\beta_2,\zeta)]\right\};$$

$$S_2(\zeta)=2s^{-1}\left\{2s_1K_0(\beta_1+\beta_2,\zeta)-\frac{1}{2}(s_1+s_2)[s_1s_2^{-1}K_0(2\beta_2,\zeta)+K_0(2\beta_1,\zeta)]\right\};$$

$$R_2(\zeta)=s^{-1}(s_1+s_2)\left\{K_{-1}(\beta_1+\beta_2,\zeta)-\frac{1}{2}[K_{-1}(2\beta_1,\zeta)+K_{-1}(2\beta_2,\zeta)];\right.$$

$$K_0(p,\zeta)=p(\zeta^2+p^2)^{-1};\qquad K_{-1}(p,\zeta)=-(2\beta)^{-1}\ln(\zeta^2+p^2);$$

$$K_1(p,\zeta)=\beta(p^2-\zeta^2)(\zeta^2+p^2)^{-2}\quad(\operatorname{Im}\zeta=0,\quad\beta=ha^{-1},\quad\beta_i=w_i\beta,$$

$$\operatorname{Re}\beta_i>0,\quad i=1,2;\quad s_1=l_1w_2,\quad s_2=l_2w_1,\quad s=s_1-s_2).$$

The Bubnov–Galerkin method is used for a numerical investigation of the eigenvalue problem (3.2.11). Selected as coordinate functions is the system of real power-law functions 1, x, x^2, ..., that corresponds to the expansion of real and imaginary parts of the desired functions in the mentioned coordinate system. The coefficients in the expansions of the unknown complex-values functions in the mentioned coordinate system are complex.

The investigations were performed for the most utilized spatial theories of plasticity deformation theory [28, 56], and flow theory [61].

Deformation theory with a power law

$$\sigma_u^0=A(\varepsilon_u^0)^k \tag{3.2.12}$$

is the relation between the stress and strain intensity. For the law (3.2.12)

$$E_k/E_c=k,\quad \sigma_{11}^0/E_c=2\varepsilon_{11}^0. \tag{3.2.13}$$

Dependences of the relative critical shortening $\varepsilon_1=1-\lambda_1$ and the critical dimensionless compressive stress $\sigma=\sigma_{11}{}^0/E_c$ on the quantity k [see (3.2.12)] are represented in Fig. 37 for different values of $\beta=h\alpha^{-1}$. Let us note that $\varepsilon_1=-\varepsilon_{11}{}^0$ for small subcritical deformations. The same dependences are represented in Fig. 38 in a form normalized to the critical values of the surface instability $\varepsilon_1{}^*$ and σ^*. A graph of the dependences ε_1 and σ on the relative distance from the crack to the free surface $\beta=h\alpha^{-1}$ is given in Figs. 39 and 40 for pure aluminum ($k\approx 0.23$; $\sigma^*=-0.212$; $\varepsilon_1{}^*=-0.106$) for different ranges of variation of β.

As follows from the results presented, the critical values of the parameters ε_1, σ in the range of variation of β of order 0.1-0.25 are an order and more below the values corresponding to the case of an isolated crack in an infinite material [19]. As $\beta\to\infty$ the crit-

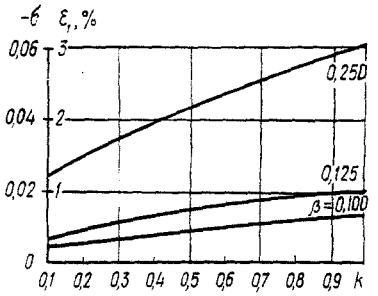

Fig. 37

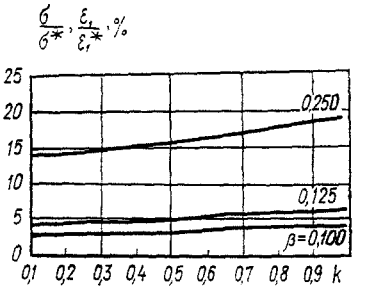

Fig. 38

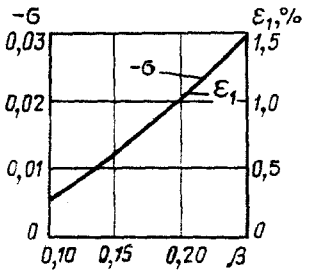

Fig. 39

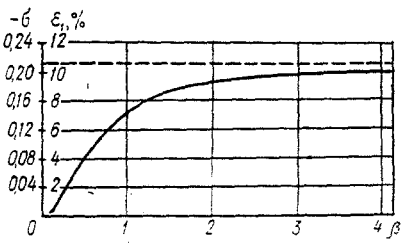

Fig. 40

ical values of ε_1, σ tend to the values ε_1^*, σ^*. Let us also note that material fracture within the framework of deformation theory with the law (3.2.12) occurs for lower loads than for an elastic material (the case k = 1 corresponds to an elastic incompressible material) for the considered values of β. Let us note the sufficiently essential dependence of the critical values of σ, ε_1 on the parameter k.

Flow theory with the associated flow law with loading functions describes translational hardening

$$f(\sigma, \varepsilon^p) = (\hat{\sigma}_0^{ij} - c\varepsilon_{p0}^{ij})(\hat{\sigma}_{ij}^0 - c\varepsilon_{ij}^{p0}) - 2k^2 = 0 \qquad (3.2.14)$$

(c, k are material constants determined by test, $\hat{\sigma}_{ij}{}^0$ are stress deviator components, and $\varepsilon_{ij}{}^{p0}$ are plastic deformations).

The numerical investigation was performed for specific mountain rocks taking into account that such problems are sufficiently typical in geomechanics under mountain relief conditions and tectonic force action. The mountain impact phenomenon can apparently be explained by the fracture mechanism within the framework of the criterion taken. Results of investigations for the relative distance $\beta = ha^{-1} = 0.125$ between the crack and the boundary of the massif are presented in Table 7 for argillite and sandstone: σ, $\varepsilon_{11}{}^0$, $\varepsilon_{11}{}^{e0}$, $\varepsilon_{11}{}^{p0}$ are critical values, respectively, of the compressive stress $\sigma_{11}{}^0$ (referred to the elastic modulus E), the total, elastic, and plastic deformations; σ^*, ε^*, ε_*^e, ε_*^p are the same quantities corresponding to a surface instability (and also to the case of an isolated crack in an infinte material); σ_H, ε_H are the unmeasured compressive stress and deformation corresponding to passage of the massif into the plastic state. The nature of the convergence of the method being used (depending on the number N of coordinate functions) is illustrated by the data in Table 8 (the first and second rows), where critical values are presented for the total deformations $\varepsilon_{11}{}^0$ for argillite (to third decimal place accuracy).

The material constants E, c, k are determined for the mountain rocks mentioned on the basis of test results on triaxial loading of continuous (without macrocracks) circular cylindrical specimens (realized was a class of states with principle stresses $\sigma_1 = \sigma_2 = C\sigma_3$ (C = const), longitudinal compression with lateral squeezing). Presented in Table 9 are maximal values (in absolute value) of the principle critical stresses and strains σ_{max}, ε_{max} obtained in the problem under consideration, and the maximal values of the principal stresses and strains σ_{max}^{test}, corresponding to the fracture of continuous specimens in the above-mentioned tests for different values of C. Let us note that since the stress–strain states in the tests were close to the states under uniaxial compression (C = 0) and biaxial uniform compression was realized in the problem under consideration, comparison of the theoretical

TABLE 7

Material	Argillite	Sandstone
σ	—0,015	—0,015
ε_{11}^{0}	—0,010	—0,009
ε_{11}^{e0}	—0,007	—0,007
ε_{11}^{p0}	—0,003	—0,002
σ^*	—0,276	—0,278
ε^*	—0,226	—0,219
ε_*^e	—0,138	—0,139
ε_*^p	—0,088	—0,080
$\sigma_н$	—0,006	—0,009
$\varepsilon_н$	—0,003	—0,004

TABLE 8

N	1	2	3	4	5	6
ε^0_{11}	—0,189	—0,016	—0,015	—0,010	—0,010	—0,010
ε_1	0,243	0,050	0,051	0,045	0,045	0,045

TABLE 9

Material	$\sigma_{max}\cdot 10^8$ Pa	$\varepsilon_{max}\cdot 10^{-2}$	c	$\sigma^{test}_{max}\cdot 10^8$ Pa	$\varepsilon^{test}_{max}\cdot 10^{-2}$
Argillite	3,0	2,0	0	1,1	0,6
			0,19	2,2	1,5
			0,316	4,4	2,1
Sandstone	4,5	1,9	0	1,4	0,6
			0,116	4,0	1,4
			0,227	10,2	3,1

and experimental values in Table 9 in this case is provisional in nature and affords a possibility for comparing just the orders of the obtained theoretical and experimental fracture loads.

The data presented in Table 7 and Table 8 (first and second rows) and their comparison with results for an elastic material show the following: for the value $\beta = 0.125$ considered the massif goes over into the plastic state before fracture of the massif can occur according to a purely elastic mechanism within the framework of the fracture criterion assumed.

Fracture of Plastic Massifs under Compression Along Two Parallel Macrocracks. Plane (under uniaxial compression) and axisymmetric (under biaxial uniform compression) problems are examined in [70] and [25, 38, 39]. An approach analogous to that described above is used (see the previous section) to obtain resolving systems of integral equations with complex-valued kernels and desired functions on the basis of the formalism developed for real functions.

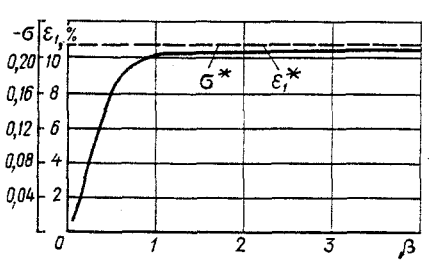

Fig. 41

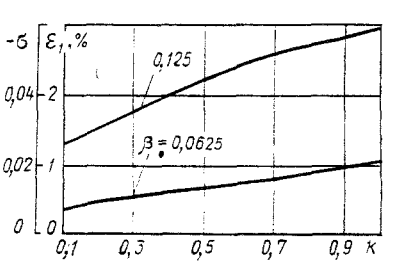

Fig. 42

TABLE 10

Material	β	$-\sigma$	$-\varepsilon_{11}^{0}$	$-\varepsilon_{11}^{e0}$	$-\varepsilon_{11}^{p0}$
Argillite	0,0625	0,0148	0,0107	0,0074	0,0033
	0,1	0,0351	0,0270	0,0176	0,0094
	0,125	0,0500	0,0393	0,0250	0,0143
Sandstone	0,0625	0,0158	0,0100	0,0079	0,0021
	0,1	0,0358	0,0260	0,0179	0,0081
	0,125	0,0509	0,0380	0,0255	0,0125

The plane problem [70] of compression along two parallel cracks of length 2a and distance 2h between cracks is reduced, separately for the bending and symmetric buckling modes, to a resolving system of equations of the first kind with a logarithmic singularity of the type (2.1.21) (taking into account that the desired functions and kernels are complex-valued functions and also the simplifications needed to use the second modification of the theory of small subcritical deformations).

Axisymmetric problems [25, 38, 39] also reduce first to problems for a half-space, separately for the symmetric and bending buckling modes, and then to a system of Fredholm integral equations of the second kind of the type (2.2.12) for complex-valued functions. The numerical investigation is performed for deformation theory with a power law relating the stress and strain intensities and flow theory with the loading function (3.2.14).

Deformation Theory. Critical values $\varepsilon_1 = 1 - \lambda_1$ for $\beta = h a^{-1} = 0.25$ (a is the radius of coaxial cracks and 2h is the distance between them) are presented in Table 8 (the first and third columns) depending on the number N of coordinate functions used for pure aluminum ($k \approx 0.23$). Fig. 41 illustrates the dependences of ε_1 and σ (see above) on the quantity β for pure aluminum ($k \approx 0.23$; $\sigma^* = -0.212$; $\varepsilon_1^* = 0.106$).

The dependences of ε_1, σ on the magnitude of the exponent k in the law (3.2.12) are represented in Fig. 42 for the values $\beta = 0.0625$, 0.125.

Results of a numerical investigation for flow theory with translational hardening in application to mountain rocks (see the previous section) are presented in Table 10. Here $\sigma = \sigma_{11}^{0}/E$ is the unmeasured compressive stress, ε_{11}^{0}, ε_{11}^{e0}, ε_{11}^{p0} are the total, elastic, and plastic deformations.

For a sufficiently small distance between the cracks the critical loads differ substantially from the load for an isolated crack in an infinite material (an order and more lower). Compared with the case of a near-surface crack in a half-space, higher values of the critical relative shortenings and stresses are obtained, as agrees with reasoning of a physical nature.

CONCLUSIONS

The results elucidated in this paper and in [A. N. Guz' and V. M. Nazarenko, "Fracture mechanics of materials under compression along cracks (Survey). Highly-elastic material," Prikl. Mekh., 25, No. 9, 3-32 (1989)] of investigations on compression of materials along defects of crack type are exact since they are obtained within the framework of rigorous three-dimensional linearized formulations. Let us note that the fact that the mentioned result are standards for approximate approaches is of independent value.

The investigations performed whose survey is represented above should be considered the beginning of a study of problems of material fracture under compression along cracks in a rigorous formulation (within the framework of the linearized mechanics of deformable bodies).